PHYSICAL REVIEW D **85,** 115026 (2012)

Study of $B_c \to D_s^* \ell^+ \ell^-$ in a single universal extra dimension

U. O. Yilmaz*

Physics Department, Karabuk University, 78100 Karabuk, Turkey

(Received 3 May 2012; published 26 June 2012)

The rare semileptonic $B_c \to D_s^* \ell^+ \ell^-$ decay is studied in the scenario of the universal extra dimension model with a single extra dimension in which the inverse of the compactification radius R is the only new parameter. The sensitivity of differential branching ratio, total branching ratio, polarization, and forward-backward asymmetries of final state leptons, both for muon and tau, to the compactification parameter is presented. For some physical observables, the uncertainty on the form factors and resonance contributions have been considered in the calculations. The obtained results, compared with the available data, show that new contributions appear due to the extra dimension.

DOI: 10.1103/PhysRevD.85.115026 PACS numbers: 12.60.−i, 13.20.Fc, 13.88.+e

I. INTRODUCTION

Flavor-changing neutral current (FCNC) $b \to s$, d transitions which occur at the loop level in the standard model (SM) provide us a powerful tool to test the SM and also a frame to study physics beyond the SM. After the observation of $b \to s\gamma$ [1], these transitions became more attractive and since then rare radiative, leptonic, and semileptonic decays of $B_{u,d,s}$ mesons have been intensively studied [2]. Among these decays, semileptonic decay channels are significant because of having relatively larger branching ratios. The experimental data for exclusive $B \to K^{(*)} \ell^+ \ell^-$ also increased the interest in these decays. These studies will be even more complete if similar studies for B_c, discovered by the CDF Collaboration [3], are also included.

The B_c meson is the lowest bound state of two heavy quarks, bottom b and charm c, with explicit flavor that can be compared with the $c\bar{c}$ and $b\bar{b}$ bound states which have implicit flavors. The implicit-flavor states decay strongly and electromagnetically whereas the B_c meson decays weakly. $B_{u,d,s}$ are described very well in the framework of the heavy quark limit, which gives some relations between the form factors of the physical processes. In the case of the B_c meson, the heavy flavor and spin symmetries must be reconsidered because of heavy b and c. On the experimental side of the decay, for example, at LHC, $10^{10} B_c$ events per year are estimated [4,5]. This reasonable number is stimulating the work on the B_c phenomenology and this possibility will provide information on rare B_c decays as well as CP violation and polarization asymmetries.

In the rare B meson decays, the effects of the new physics may appear in two different manners, either through the new contributions to the Wilson coefficients existing in the SM or through the new structures in the effective Hamiltonian which are absent in the SM.

Considering different models beyond the SM, extra dimensions are specially attractive because of including gravity and other interactions, giving hints to the hierarchy problem and a connection with string theory. Those with universal extra dimensions (UED) are of special interest because all the SM particles propagate in extra dimensions, the compactification of which allows Kaluza-Klein (KK) partners of the SM fields in the four-dimensional theory and also KK modes without corresponding the SM partners [6–9]. Throughout the UED, a simpler scenario with a single universal extra dimension is the Appelquist-Cheng-Dobrescu (ACD) model [10]. The only additional free parameter with respect to the SM is the inverse of the compactification radius, $1/R$. In the particle spectrum of the ACD model, there are infinite towers of KK modes, and the ordinary SM particles are presented in the zero mode.

This is the only parameter where putting a theoretical or experimental restriction on it has been attempted. Tevatron experiments put the bound $1/R \geq 300$ GeV. Analysis of the anomalous magnetic moment and $B \to X_s \gamma$ [11] also lead to the bound $1/R \geq 300$ GeV. In the study of $B \to K^* \gamma$ decay [12], the results restrict R to be $1/R \geq 250$ GeV. Also, in [13] this bound is $1/R \geq 330$ GeV. In two recent works, the theoretical study of $B \to K \eta \gamma$ matches with the experimental data if $1/R \geq 250$ GeV [14] and using the experimental result [15] and theoretical prediction on the branching ratio of $\Lambda_b \to \Lambda \mu^+ \mu^-$, the lower bound was obtained to be approximately $1/R \sim 250$ GeV [16]. In this work, we will consider $1/R$ from 200 GeV up to 1000 GeV, however, under above consideration the $1/R = 250$–350 GeV region will be taken as the more common bound region. In the literature, the effective Hamiltonian of several FCNC processes [17,18], semileptonic and radiative decays have been investigated in the ACD model [19–29].

Concentrating on $B_c \to D_s^* \ell^+ \ell^-$ decay, it has been studied by using the model independent effective Hamiltonian [30], in supersymmetric models [31] and with fourth generation effects [32]. Also in [33], the UED effects on the branching ratio and helicity fractions of the final state D^* meson were calculated using the form factors obtained through the Ward identities for this

*uoyilmaz@karabuk.edu.tr

process. The weak annihilation contribution in addition to the FCNC transitions were taken into account. We will, however, only consider the FCNC transitions and calculate the lepton asymmetries adding the resonance contributions.

The main aim of this paper is to find the effects of the ACD model on some physical observables related to the $B_c \to D_s^* \ell^+ \ell^-$ decay, and while doing this we also give the behavior of these observables by a couple of figures in the SM. Measurement of final state lepton polarizations is a useful way to search new physics beyond the SM. Another tool is the study of forward-backward asymmetry (A_{FB}), especially the position of the zero value of A_{FB} is very sensitive to the new physics. In addition to a differential decay rate and branching ratio, we study forward-backward asymmetry and the polarization of final state leptons, including resonance contributions and the uncertainty on the form factors in as many as possible cases. We analyze these observables in terms of the compactification factor and the form factors. The form factors for $B_c \to D_s^* \ell^+ \ell^-$ have been calculated using the light front, constitute quark models [34], the relativistic constituent quark model [35], relativistic quark model [36], and light-cone quark model [37]. In this work, we will use the form factors calculated in the three-point QCD sum rules [38].

The paper is organized as follows. In Sec. II, we give the effective Hamiltonian for the quark-level process $b \to s\ell^+\ell^-$ and mention briefly the Wilson coefficients in the ACD model (a detailed discussion is given in the Appendix). We derive the matrix element using the form factors and calculate the decay rate in Sec. III. In Sec. VI, we present the forward-backward asymmetry and Sec. V is devoted to lepton polarizations. In the last section, we introduce our conclusions.

II. EFFECTIVE HAMILTONIAN AND WILSON COEFFICIENTS

The quark-level transition of $B_c \to D_s^* \ell^+ \ell^-$ decay is governed by $b \to s\ell^+\ell^-$ and given by the following effective Hamiltonian in the SM [39]:

$$\mathcal{H}_{\text{eff}} = \frac{G_F \alpha}{\sqrt{2}\pi} V_{tb} V_{ts}^* \Big[C_9^{\text{eff}} (\bar{s}\gamma_\mu L b)\bar{\ell}\gamma^\mu + C_{10}(\bar{s}\gamma_\mu L b)\bar{\ell}\gamma^\mu\gamma_5 \ell - 2C_7^{\text{eff}} m_b \Big(\bar{s} i\sigma_{\mu\nu}\frac{q^\nu}{q^2} R b\Big)\bar{\ell}\gamma^\mu \ell \Big], \quad (1)$$

where q is the momentum transfer, $L, R = (1 \pm \gamma_5)/2$ and C_is are the Wilson coefficients evaluated at the b quark mass scale.

The coefficient C_9^{eff} has perturbative and resonance contributions. So, C_9^{eff} can be written as

$$C_9^{\text{eff}}(\mu) = C_9(\mu)\Big(1 + \frac{\alpha_s(\mu)}{\pi}\omega(s')\Big) + Y(\mu, s') + C_9^{\text{res}}(\mu, s'), \quad (2)$$

where $s' = q^2/m_b^2$.

The perturbative part, coming from the one-loop matrix elements of the four-quark operators, is

$$\begin{aligned} Y(\mu, s') = {} & h(y, s')[3C_1(\mu) + C_2(\mu) + 3C_3(\mu) + C_4(\mu) \\ & + 3C_5(\mu) + C_6(\mu)] - \tfrac{1}{2}h(1, s')(4C_3(\mu) + 4C_4(\mu) \\ & + 3C_5(\mu) + C_6(\mu)) - \tfrac{1}{2}h(0, s')[C_3(\mu) + 3C_4(\mu)] \\ & + \tfrac{2}{9}(3C_3(\mu) + C_4(\mu) + 3C_5(\mu) + C_6(\mu)), \end{aligned} \quad (3)$$

with $y = m_c/m_b$. The explicit forms of the functions $\omega(s')$ and $h(y, s')$ are given in [40,41].

The resonance contribution due to the conversion of the real $c\bar{c}$ into lepton pair can be done by using a Breit-Wigner shape as [42],

$$\begin{aligned} C_9^{\text{res}}(\mu, s') = {} & -\frac{3}{\alpha_{em}^2}\kappa \sum_{V_i = \psi_i} \frac{\pi\Gamma(V_i \to \ell^+\ell^-) m_{V_i}}{s m_b^2 - m_{V_i}^2 + i m_{V_i}\Gamma_{V_i}} \\ & \times [3C_1(\mu) + C_2(\mu) + 3C_3(\mu) \\ & + C_4(\mu) + 3C_5(\mu) + C_6(\mu)]. \end{aligned} \quad (4)$$

The normalization is fixed by the data in [43] and the phenomenological parameter κ is taken 2.3 to produce the correct branching ratio $\text{BR}(B \to J/\psi K^* \to K^*\ell^+\ell^-) = \text{BR}(B \to J/\psi K^*)B(J/\psi \to \ell^+\ell^-)$.

In the ACD model, there are no new operators, therefore, new physics contributions appear by modifying the Wilson coefficients available in the SM. In this model, the Wilson coefficients can be written in terms of some periodic functions, as a function of compactification factor $1/R$. The function $F(x_t, 1/R)$ generalizes the $F_0(x_t)$ SM functions according to

$$F(x_t, 1/R) = F_0(x_t) + \sum_{n=1}^{\infty} F_n(x_t, x_n), \quad (5)$$

where $x_t = m_t^2/m_W^2$, $x_n = m_n^2/m_W^2$ with the mass of KK particles $m_n = n/R$. $n = 0$ corresponds to the ordinary SM particles. The modified Wilson coefficients in the ACD model, taken place in many works in the literature, are discussed in the Appendix.

Briefly, for C_9, in the ACD model and in the naive dimensional regularization (NDR) scheme, we have

$$\begin{aligned} C_9(\mu, 1/R) = {} & P_0^{\text{NDR}} + \frac{Y(x_t, 1/R)}{\sin^2\theta_W} - 4Z(x_t, 1/R) \\ & + P_E E(x_t, 1/R). \end{aligned} \quad (6)$$

Instead of C_7, a normalization scheme independent effective coefficient C_7^{eff} can be written as

$$\begin{aligned} C_7^{\text{eff}}(\mu, 1/R) = {} & \eta^{16/23} C_7(\mu_W, 1/R) + \frac{8}{3}(\eta^{14/23} - \eta^{16/23}) C_8 \\ & \times (\mu_W, 1/R) + C_2(\mu_W, 1/R)\sum_{i=1}^{8} h_i \eta^{a_i}. \end{aligned} \quad (7)$$

The Wilson coefficient C_{10} is independent of scale μ and given by

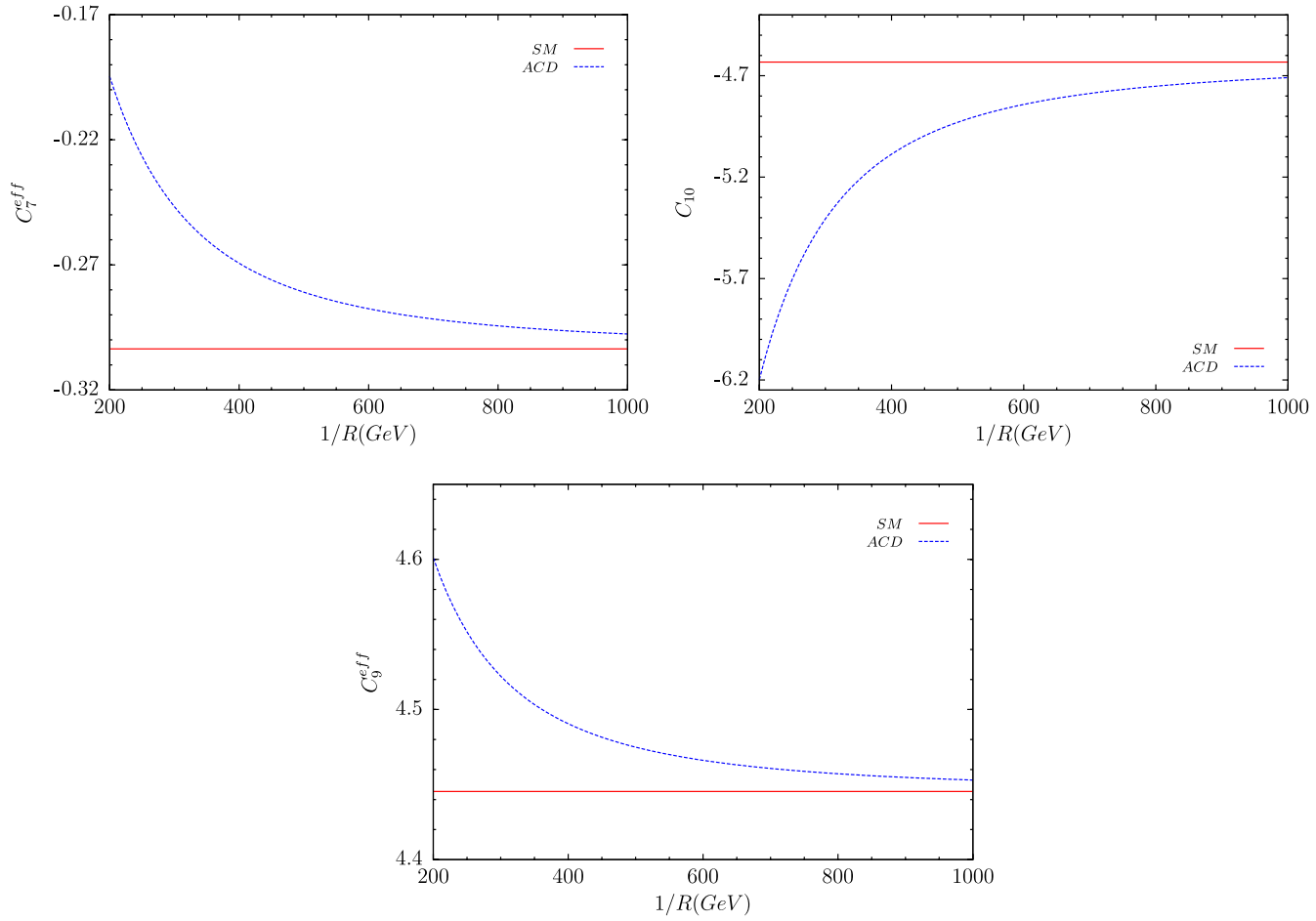

FIG. 1 (color online). The variation of Wilson coefficients with respect to $1/R$ at $q^2 = 14\ \mathrm{GeV}^2$ for the normalization scale $\mu = 4.8$ GeV. (C_9^{eff} does not include resonance contributions.)

$$C_{10}(1/R) = -\frac{Y(x_t, 1/R)}{\sin^2\theta_W}. \tag{8}$$

The Wilson coefficients differ considerably from the SM values for small R. The variation of modified Wilson coefficients with respect to $1/R$ at $q^2 = 14\ \mathrm{GeV}^2$, in which the normalization scale is fixed to $\mu = \mu_b \simeq 4.8$ GeV, is given in Fig. 1. The suppression of $|C_7^{\mathrm{eff}}|$ for $1/R =$ 250–350 GeV amounts to 75%–86% relative to the SM value. $|C_{10}|$ is enhanced by 23%–13%. The impact of the ACD on $|C_9^{\mathrm{eff}}|$ is very small. For $1/R \gtrsim 600$ GeV, the difference is less than 5%.

III. MATRIX ELEMENTS AND DECAY RATE

The hadronic matrix elements in the exclusive $B_c \to D_s^* \ell^+ \ell^-$ decay can be obtained by sandwiching the quark-level operators in the effective Hamiltonian between the initial and the final state mesons. The nonvanishing matrix elements are parameterized in terms of the form factors as follows: [44,45]

$$\langle D_s^*(p_{D_s^*}, \varepsilon)|\bar{s}\gamma_\mu(1-\gamma_5)b|B_c(p_{B_c})\rangle = -\epsilon_{\mu\nu\alpha\beta}\varepsilon^{*\nu}p_{D_s^*}^{\alpha}q^{\beta}\frac{2V(q^2)}{m_{B_c}+m_{D_s^*}} - i\varepsilon_\mu^*(m_{B_c}+m_{D_s^*})A_1(q^2)$$
$$+ i(p_{B_c}+p_{D_s^*})_\mu(\varepsilon^* q)\frac{A_2(q^2)}{m_{B_c}+m_{D_s^*}} + iq_\mu(\varepsilon^* q)\frac{2m_{D_s^*}}{q^2}[A_3(q^2)-A_0(q^2)], \tag{9}$$

and

$$\langle D_s^*(p_{D_s^*}, \varepsilon)|\bar{s}i\sigma_{\mu\nu}q^\nu(1+\gamma_5)b|B_c(p_{B_c})\rangle = 2\epsilon_{\mu\nu\alpha\beta}\varepsilon^{*\nu}p_{D_s^*}^{\alpha}q^{\beta}T_1(q^2) + i[\varepsilon_\mu^*(m_{B_c}^2 - m_{D_s^*}^2) - (p_{B_c}+p_{D_s^*})_\mu(\varepsilon^* q)]T_2(q^2)$$
$$+ i(\varepsilon^* q)\left[q_\mu - (p_{B_c}+p_{D_s^*})_\mu\frac{q^2}{m_{B_c}^2 - m_{D_s^*}^2}\right]T_3(q^2), \tag{10}$$

where $q = p_{B_c} - p_{D_s^*}$ is the momentum transfer and ε is the polarization vector of D_s^* meson.

The relation between the form factors $A_1(q^2), A_2(q^2)$ and $A_3(q^2)$ can be stated as

$$A_3(q^2) = \frac{m_{B_c} + m_{Ds^*}}{2m_\phi} A_1(q^2) - \frac{m_{B_c} - m_{D^*}}{2m_\phi} A_2(q^2),$$

and in order to avoid kinematical singularity in the matrix element at $q^2 = 0$, it is assumed that $A_0(0) = A_3(0)$ and $T_1(0) = T_2(0)$ [45].

Using the effective Hamiltonian and matrix elements in Eqs. (9) and (10), the transition amplitude for $B_c \to D_s^* \ell^+ \ell^-$ is written as

$$\mathcal{M}(B_c \to D_s^* \ell^+ \ell^-) = \frac{G\alpha}{2\sqrt{2}\pi} V_{tb} V_{ts}^* \{\bar{\ell}\gamma^\mu \ell[-2A\epsilon_{\mu\nu\alpha\beta}\varepsilon^{*\nu} p_{D_s^*}^\alpha q^\beta - iB\varepsilon_\mu^* + iC(\varepsilon^* q)(p_{B_c} + p_{D_s^*})_\mu + iD(\varepsilon^* q) q_\mu]$$
$$+ \bar{\ell}\gamma^\mu \gamma_5 \ell[-2E\epsilon_{\mu\nu\alpha\beta}\varepsilon^{*\nu} p_{D_s^*}^\alpha q^\beta - iF\varepsilon_\mu^* + iG(\varepsilon^* q)(p_{B_c} + p_{D_s^*})_\mu + iH(\varepsilon^* q) q_\mu]\}, \quad (11)$$

with the auxiliary functions

$$A = C_9^{\text{eff}} \frac{V(q^2)}{m_{B_c} + m_{D_s^*}} + \frac{2m_b}{q^2} C_7^{\text{eff}} T_1(q^2), \quad B = C_9^{\text{eff}} (m_{B_c} + m_{D_s^*}) A_1(q^2) + \frac{2m_b}{q^2} C_7^{\text{eff}} (m_{B_c}^2 - m_{D_s^*}^2) T_2(q^2),$$
$$C = C_9^{\text{eff}} \frac{A_2(q^2)}{m_{B_c} + m_{D_s^*}} + \frac{2m_b}{q^2} C_7^{\text{eff}} (T_2(q^2) + \frac{q^2}{m_{B_c}^2 - m_{D_s^*}^2} T_3(q^2)), \quad D = 2C_9^{\text{eff}} \frac{m_{D_s^*}}{q^2} (A_3(q^2) - A_0(q^2)) - 2\frac{m_b}{q^2} C_7^{\text{eff}} T_3(q^2), \quad (12)$$
$$E = C_{10} \frac{V(q^2)}{m_{B_c} + m_{D_s^*}}, \quad F = C_{10}(m_{B_c} + m_{D_s^*}) A_1(q^2), \quad G = C_{10} \frac{A_2(q^2)}{m_{B_c} + m_{D_s^*}}, \quad H = 2C_{10} \frac{m_{D_s^*}}{q^2} (A_3(q^2) - A_0(q^2)).$$

Integrating over the angular dependence of the double differential decay rate, the following dilepton mass spectrum is obtained:

$$\frac{d\Gamma}{ds} = \frac{G^2 \alpha^2 m_{B_c}}{2^{12} \pi^5} |V_{tb} V_{ts}^*|^2 \sqrt{\lambda} v \Delta_{D_s^*}, \quad (13)$$

where $s = q^2/m_{B_c}^2$, $\lambda = 1 + r^2 + s^2 - 2r - 2s - 2rs$, $r = m_{D_s^*}^2/m_{B_c}^2$, $v = \sqrt{1 - 4m_\ell^2/s m_{B_c}^2}$ and

$$\Delta_{D_s^*} = \frac{8}{3}\lambda m_{B_c}^6 s[(3 - v^2)|A|^2 + 2v^2|E|^2] + \frac{1}{r}\lambda m_{B_c}^4 \Big[\frac{1}{3}\lambda m_{B_c}^2 (3 - v^2)|C|^2 + m_{B_c}^2 s^2 (1 - v^2)|H|^2 + \frac{2}{3}[(3 - v^2)(r + s - 1)$$
$$- 3s(1 - v^2)]\text{Re}[FG^*] + 2m_{B_c}^2 s(1 - r)(1 - v^2)\text{Re}[GH^*] - 2s(1 - v^2)\text{Re}[FH^*] + \frac{2}{3}(3 - v^2)(r + s - 1)\text{Re}[BC^*]\Big]$$
$$+ \frac{1}{3r}(3 - v^2) m_{B_c}^2 [(\lambda + 12rs)|B|^2 + \lambda m_{B_c}^4 [\lambda - 3s(s - 2r - 2)(1 - v^2)]|G|^2 + [\lambda + 24rsv^2]|F|^2]. \quad (14)$$

In the numerical analysis, we have used $m_{B_c} = 6.28$ GeV, $m_{D_s^*} = 2.112$ GeV, $m_b = 4.8$ GeV, $m_\mu = 0.105$ GeV, $m_\tau = 1.77$ GeV, $|V_{tb} V_{ts}^*| = 0.041$, $G_F = 1.17 \times 10^{-5}$ GeV^{-2}, $\tau_{B_c} = 0.46 \times 10^{-12}$ s, and the values that are not given here are taken from [43]. In our work, we have used the numerical values of the form factors calculated in the three-point QCD sum rules [38], in which q^2 dependencies of the form factors are given as

$$F(q^2) = \frac{F(0)}{1 + a(q^2/m_{B_c}^2) + b(q^2/m_{B_c}^2)^2},$$

and the values of parameters $F(0)$, a, and b for the $B_c \to D^*$ decay are listed in Table I.

The differential branching ratio is calculated without resonance contributions, including the uncertainty on the form factors, and with resonance contributions, and the s dependence for $1/R = 200, 350, 500$ GeV is presented in Figs. 2 and 3, respectively. The change in the differential decay rate and the difference between the SM results and the new effects can be noticed in the figures. The maximum effect is around $s = 0.25 \pm 0.05 (0.37 \pm 0.02)$ for $\mu(\tau)$ in Fig. 2. In spite of the hadronic uncertainty, for

TABLE I. B_c meson decay form factors in the three-point QCD sum rules.

	$F(0)$	a	b
V	0.54 ∓ 0.018	-1.28	-0.230
A_1	0.30 ∓ 0.017	-0.13	-0.180
A_2	0.36 ∓ 0.013	-0.67	-0.066
$\propto (A_3 - A_0)$	-0.57 ∓ 0.040	-1.11	-0.140
T_1	0.31 ∓ 0.017	-1.28	-0.230
T_2	0.33 ∓ 0.016	-0.10	-0.097
T_3	0.29 ∓ 0.034	-0.91	0.007

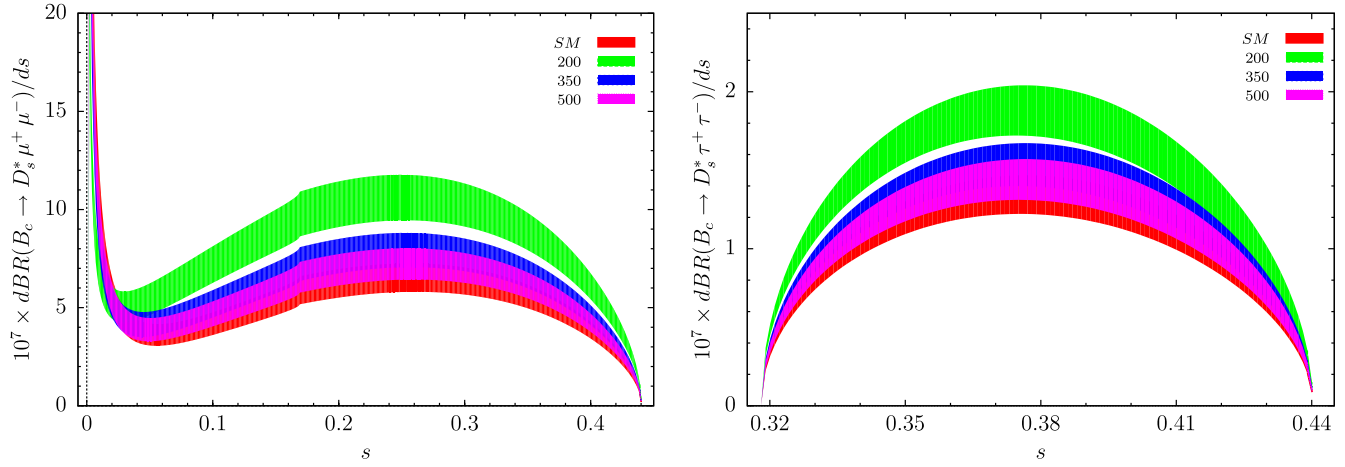

FIG. 2 (color online). The dependence of differential branching ratio on s, including the uncertainty on the form factors in the nonresonance case. (In the legend $1/R = 200, 350, 500$ GeV.)

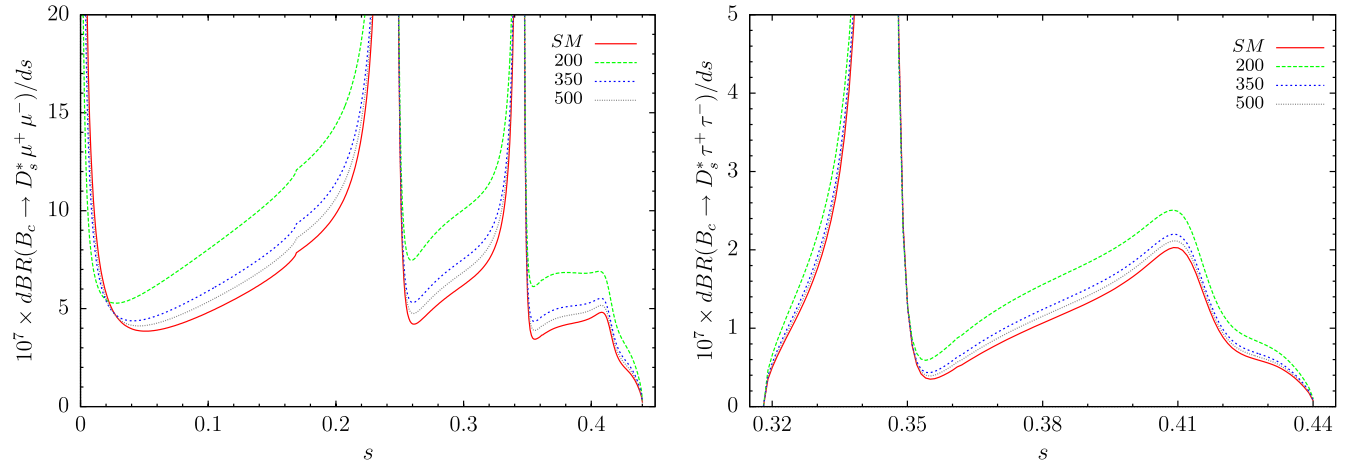

FIG. 3 (color online). The dependence of the differential branching ratio on s with the central values of the form factors including resonance contributions.

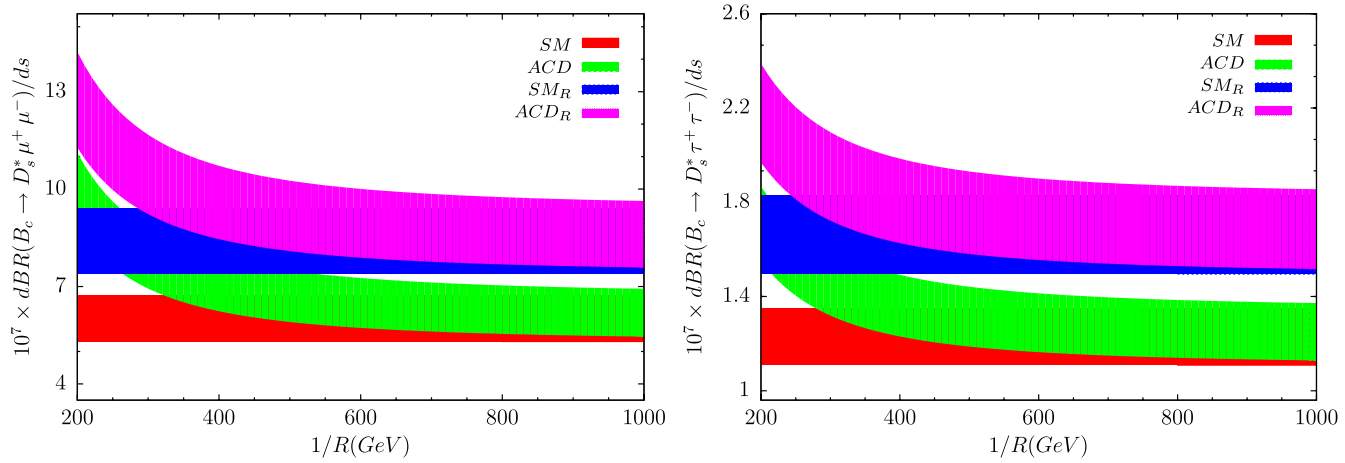

FIG. 4 (color online). The dependence of the differential branching ratio on $1/R$, with and without resonance contributions, including the uncertainty on the form factors at $s = 0.18$ for μ, and $s = 0.4$ for τ. (The subscript R in the legend represents resonance contributions.)

$1/R = 200$ GeV and 350 GeV, studying the differential decay rate can be a suitable tool for studying the effect of an extra dimension.

Supplementary to these, the $1/R$ dependence of differential branching ratio at $s = 0.18(0.4)$ for $\mu(\tau)$ is plotted in Fig. 4. Considering any given bound on the compactification factor, the effect of a universal extra dimension can be seen clearly for low values of R, with and without resonance contributions. On the other hand, when $1/R \gtrsim 600$ GeV the contribution varies between $\sim$5–8% more than the SM results.

To obtain the branching ratio, we integrate Eq. (13) in the allowed physical region. While taking the long-distance contributions into account we introduce some cuts around the J/ψ and $\psi(2s)$ resonances to minimize the hadronic uncertainties. The integration region for q^2 is divided into three parts for μ as $4m_\mu^2 \le q^2 \le (m_{J/\psi} - 0.02)^2$, $(m_{J/\psi} + 0.02)^2 \le q^2 \le (m_{\psi(2s)} - 0.02)^2$ and $(m_{\psi(2s)} + 0.02)^2 \le q^2 \le (m_{B_c} - m_{D_s^*})^2$ and for τ we have $4m_\tau^2 \le q^2 \le (m_{\psi(2s)} - 0.02)^2$ $(m_{\psi(2s)} + 0.02)^2 \le q^2 \le (m_{B_c} - m_{D_s^*})^2$, the same as in [46].

The results of the branching ratio in the SM with resonance contributions and the uncertainty on the form factors, we obtain

$$\begin{aligned} \mathrm{Br}(B_c \to D_s^* \mu^+ \mu^-) &= 2.13^{+0.27}_{-0.25} \times 10^{-7} \\ \mathrm{Br}(B_c \to D_s^* \tau^+ \tau^-) &= 1.45^{+0.15}_{-0.14} \times 10^{-8}. \end{aligned} \tag{15}$$

Observing the contribution of the ACD, the $1/R$ dependent branching ratios, including the resonance contributions and the uncertainty on the form factors, are given in Fig. 5. Comparing the SM results and our theoretical predictions on the branching ratio for both decay channels, the lower bound for $1/R$ is found to be approximately 250 GeV, which is consistent with the previously mentioned results.

As $1/R$ increases, the branching ratios approach their SM values. For $1/R \ge 550$ GeV in both channels, they become less than 5% greater than that of the SM values. Between $1/R = 250$–350 GeV the ratio is $(2.66 - 2.40)^{+0.30}_{-0.28} \times 10^{-7}$ for μ, $(1.75 - 1.61)^{+0.16}_{-0.15} \times 10^{-8}$ for the τ decay. Comparing these with the SM results, the differences are worth studying and can be considered as a signal of new physics and evidence of the existence of an extra dimension.

IV. FORWARD-BACKWARD ASYMMETRY

Another efficient tool for establishing new physics is the study of forward-backward asymmetry. The position of the zero value of A_{FB} is very sensitive to the new physics. The normalized differential form is defined for final state leptons as

$$A_{\mathrm{FB}}(s) = \frac{\int_0^1 \frac{d^2\Gamma}{dsdz} dz - \int_{-1}^0 \frac{d^2\Gamma}{dsdz} dz}{\int_0^1 \frac{d^2\Gamma}{dsdz} dz + \int_{-1}^0 \frac{d^2\Gamma}{dsdz} dz}, \tag{16}$$

where $z = \cos\theta$ and θ is the angle between the directions of ℓ^- and B_c in the rest frame of the lepton pair.

In the case of $B_c \to D_s^* \ell^+ \ell^-$, we get

$$\begin{aligned} A_{\mathrm{FB}} &= \frac{G^2 \alpha^2 m_{B_c}}{2^{12} \pi^5} |V_{tb} V_{ts}^*|^2 \frac{8 m_{B_c}^4 \sqrt{\lambda} v s (\mathrm{Re}[BE^*] + \mathrm{Re}[AF^*])}{d\Gamma/ds} \\ &= \frac{8 m_{B_c}^4 \sqrt{\lambda} v s (\mathrm{Re}[BE^*] + \mathrm{Re}[AF^*])}{\Delta_{D_s^*}}. \end{aligned} \tag{17}$$

Using the above equation, we present the variation of lepton forward-backward asymmetry with s including the uncertainty on the form factors in Fig. 6. As $1/R$ becomes smaller, a considerable difference appears between the SM and the ACD results for $s \lesssim 0.16$ in μ and $0.33 \lesssim s \lesssim 0.43$ in the τ decays. Considering the resonance contributions (the results are given in Fig. 7), one can recognize a similar situation for $s \lesssim 0.23$ and $0.32 \lesssim s \lesssim 0.44$, respectively.

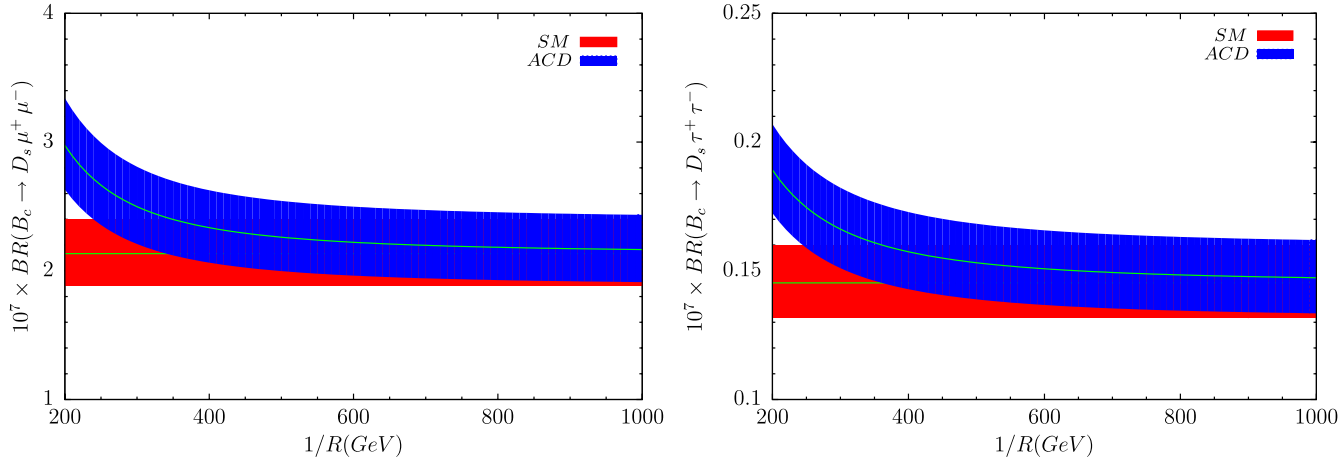

FIG. 5 (color online). The dependence of branching ratio on $1/R$, including the resonance contributions and the uncertainty on the form factors.

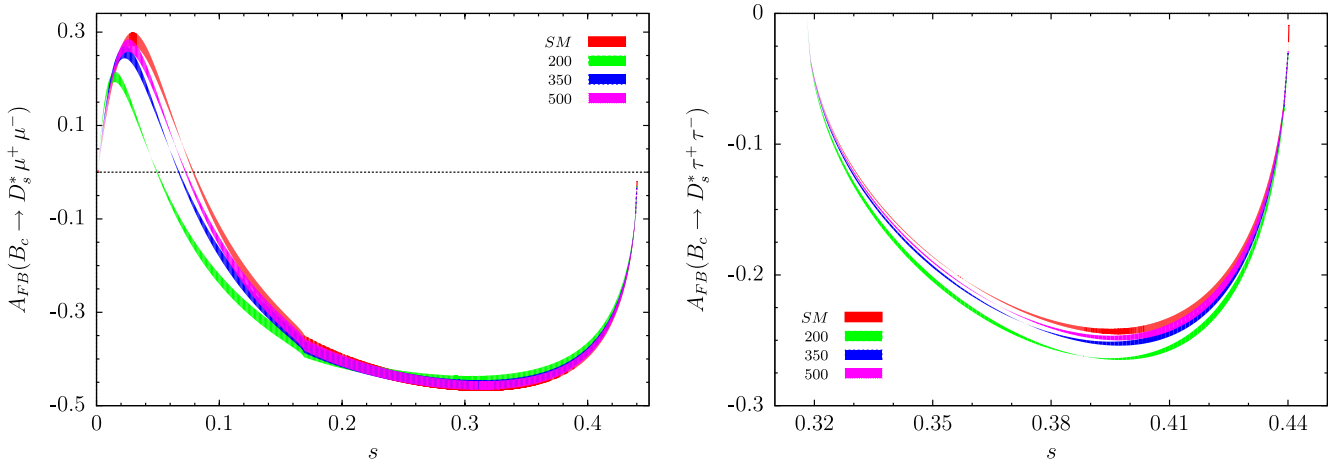

FIG. 6 (color online). The lepton forward-backward asymmetry including the uncertainty on the form factors.

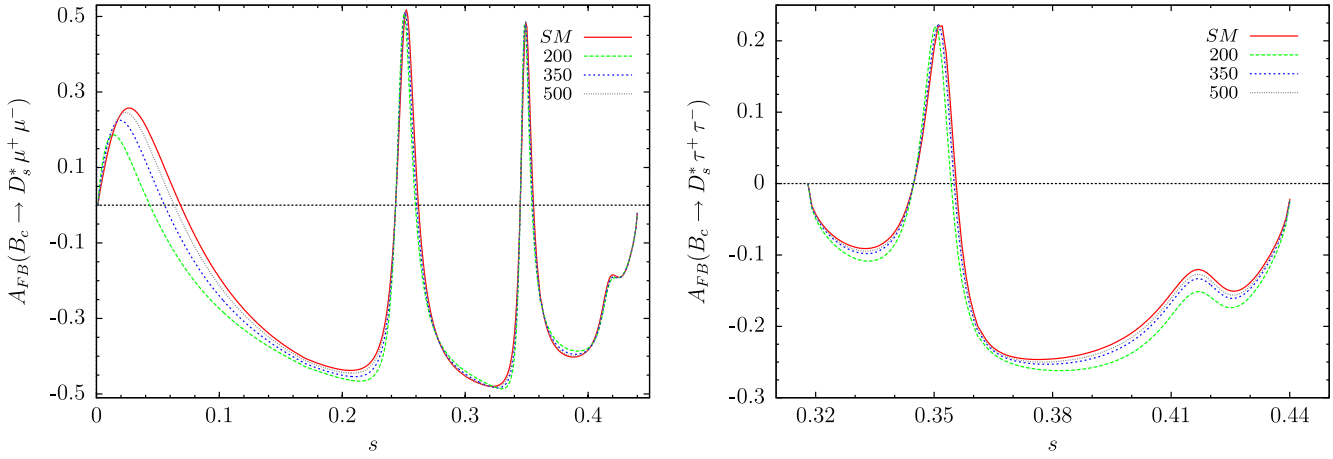

FIG. 7 (color online). The lepton forward-backward asymmetry including resonance contributions.

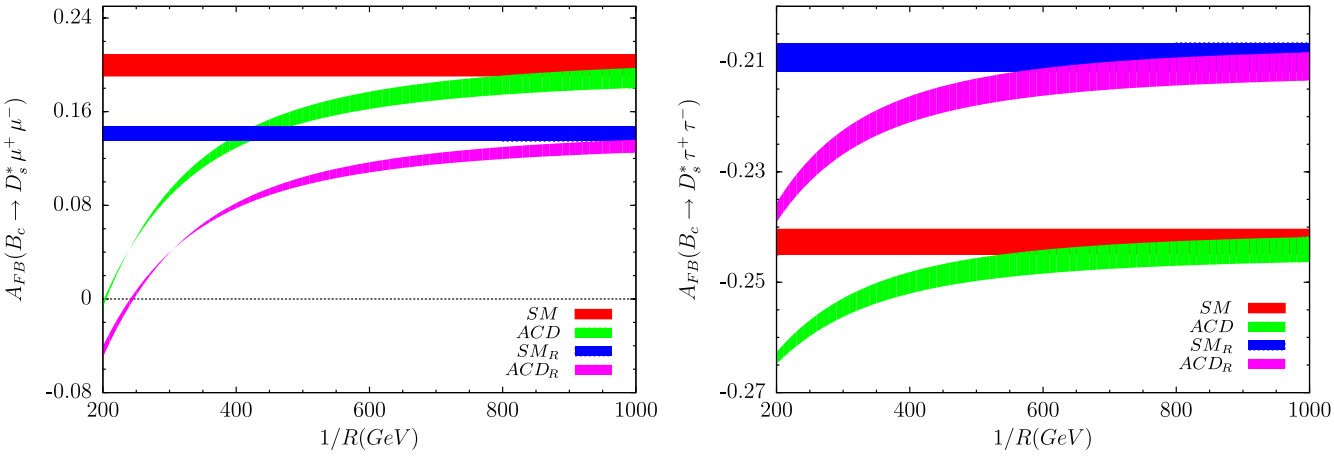

FIG. 8 (color online). The dependence of lepton forward-backward asymmetry on $1/R$ at $s = 0.05$ for μ and $s = 0.4$ for τ.

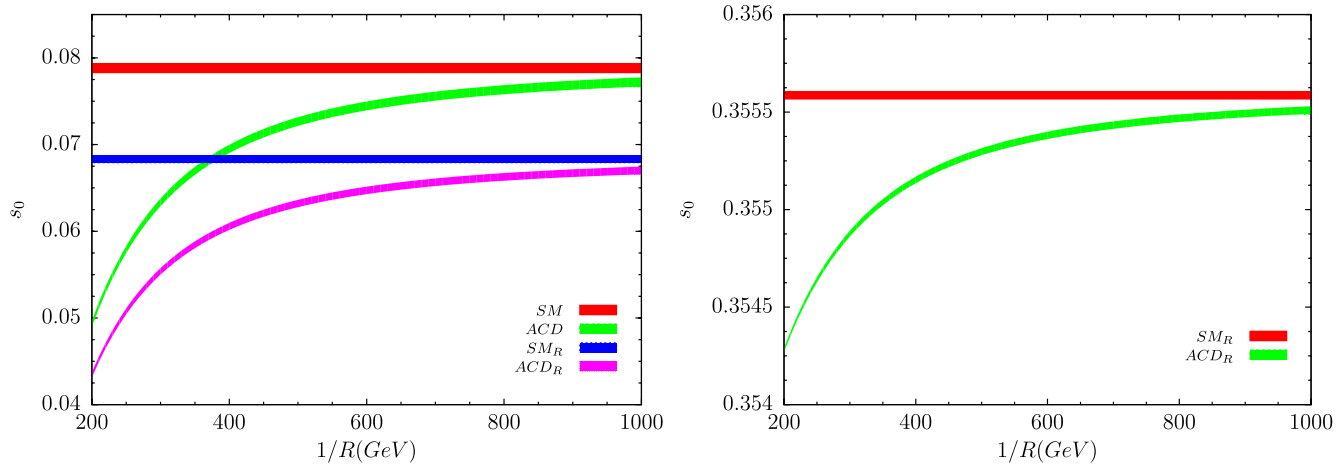

FIG. 9 (color online). The variation of the zero position of lepton forward-backward asymmetry with $1/R$.

To better understand the dependence of $A_{\rm FB}$ on $1/R$ for both lepton channels, we perform a calculation at $s = 0.05(0.4)$ for $\mu(\tau)$ and present the results in Fig. 8. In the μ channel, the UED contribution on $A_{\rm FB}$ becomes important between $1/R = 200$–600 GeV, while in the τ decay, the contribution is insignificant for $1/R \gtrsim 400$ GeV.

The position of the zero of forward-backward asymmetry, s_0, is determined numerically, and the results are presented in Fig. 9. Both plots for $B_c \to D_s^* \mu^+ \mu^-$ are for the zero point in the $s < 0.1$ region; the lower (upper) one is for the resonance (nonresonance) case, while the zero point for $B_c \to D_s^* \tau^+ \tau^-$ is because of resonance contributions. In the SM, the resonance shifts the zero point of the asymmetry, $s_0 = 0.079$, to a lower value, $s_0 = 0.068$, in $B_c \to D_s^* \mu^+ \mu^-$, i.e., further corrections could shift s_0 to smaller values [12]. As $1/R \to 200$ GeV the s_0 approaches low values for both decay channels. In the $1/R = 250$–350 GeV region, s_0 varies between (0.058–0.068) without resonance contributions and (0.051–0.058) with resonance contributions. The s_0 shift is $\sim 5\%$ of the SM value for $1/R \gtrsim 600$ GeV. The variation of s_0 for $B_c \to D_s^* \tau^+ \tau^-$ is negligible.

V. LEPTON POLARIZATION ASYMMETRIES

We will discuss the possible effects of the ACD model in lepton polarizations, as a way of searching new physics. Using the convention followed by previous works [47,48], in the rest frame of ℓ^- we define the orthogonal unit vectors S_i^-, for the polarizations of the lepton along the longitudinal, transverse, and normal directions as

$$\begin{aligned} S_L^- &\equiv (0, \vec{e}_L) = \left(0, \frac{\vec{p}_\ell}{|\vec{p}_\ell|}\right), \\ S_N^- &\equiv (0, \vec{e}_N) = \left(0, \frac{\vec{p}_{D_s^*} \times \vec{p}_\ell}{|\vec{p}_{D_s^*} \times \vec{p}_\ell|}\right), \\ S_T^- &\equiv (0, \vec{e}_T) = (0, \vec{e}_N \times \vec{e}_L), \end{aligned} \tag{18}$$

where $\vec{p}_\ell$ and $\vec{p}_{D_s^*}$ are the three momenta of ℓ^- and D_s^* meson in the center of mass (CM) frame of $\ell^+ \ell^-$ system, respectively. The longitudinal unit vector S_L^- is boosted by Lorentz transformation,

$$S_{L,CM}^{-\mu} = \left(\frac{|\vec{p}_\ell|}{m_\ell}, \frac{E_\ell \vec{p}_\ell}{m_\ell |\vec{p}_\ell|}\right), \tag{19}$$

while vectors of perpendicular directions remain unchanged under the Lorentz boost.

The differential decay rate of $B_c \to D_s^* \ell^+ \ell^-$ for any spin direction $\vec{n}^-$ of the ℓ^- can be written in the following form:

$$\frac{d\Gamma(\vec{n}^-)}{ds} = \frac{1}{2}\left(\frac{d\Gamma}{ds}\right)_0 [1 + (P_L \vec{e}_L^- + P_N^- \vec{e}_N^- + P_T^- \vec{e}_T^-) \cdot \vec{n}^-]. \tag{20}$$

Here, $(d\Gamma/ds)_0$ corresponds to the unpolarized decay rate, whose explicit form is given in Eq. (13).

The polarizations P_L^-, P_T^- and P_N^- in Eq. (20) are defined by the equation

$$P_i^-(s) = \frac{\frac{d\Gamma}{ds}(\mathbf{n}^- = \mathbf{e}_i^-) - \frac{d\Gamma}{ds}(\mathbf{n}^- = -\mathbf{e}_i^-)}{\frac{d\Gamma}{ds}(\mathbf{n}^- = \mathbf{e}_i^-) + \frac{d\Gamma}{ds}(\mathbf{n}^- = -\mathbf{e}_i^-)},$$

for $i = L, N, T$. Here, P_L^- and P_T^- represent the longitudinal and transversal asymmetries, respectively, of the charged lepton ℓ^- in the decay plane, and P_N^- is the normal component to both of them.

The explicit form of longitudinal polarization for ℓ^- is

$$\begin{aligned} P_L^- = \frac{1}{3\Delta_{D_s^*}} & 4m_{B_c}^2 v[8m_{B_c}^4 s\lambda \mathrm{Re}[AE^*] + \frac{1}{r}(12rs + \lambda)\mathrm{Re}[BF^*] \\ & - \frac{1}{r}\lambda m_{B_c}^2 (1 - r - s)[\mathrm{Re}[BG^*] + \mathrm{Re}[CF^*]] \\ & + \frac{1}{r}\lambda^2 m_{B_c}^4 \mathrm{Re}[CG^*]]. \end{aligned} \tag{21}$$

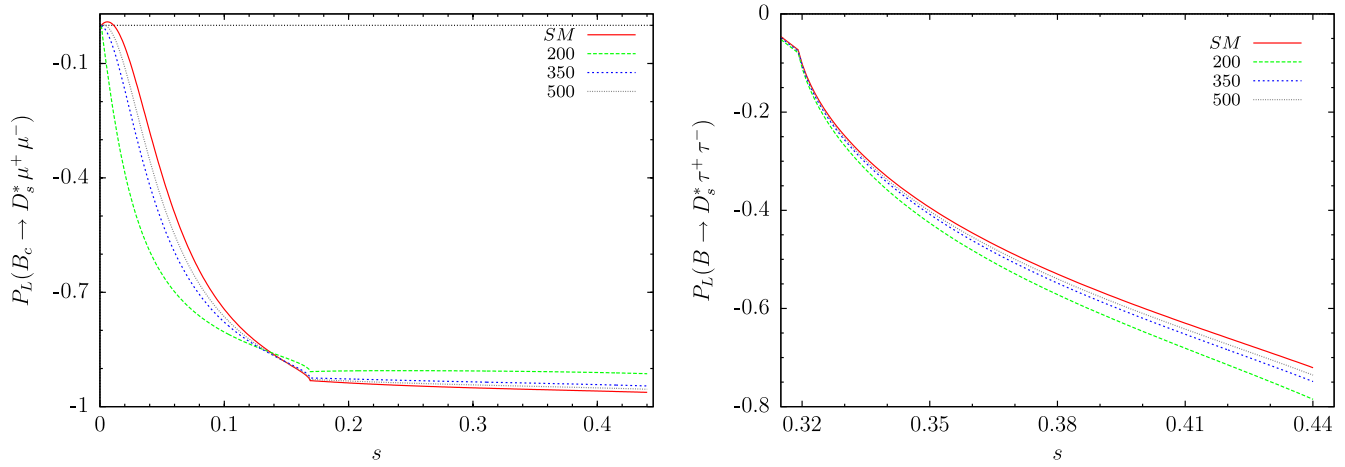

FIG. 10 (color online). The dependence of longitudinal polarization on s without resonance contributions using the central values of the form factors.

Similarly, the transversal polarization is given by

$$P_T^- = \frac{1}{\Delta_{D_s^*}} m_{B_c} m_\ell \pi \sqrt{s\lambda} \Big[-8 m_{B_c}^2 \,\mathrm{Re}[AB^*] + \frac{(1-r-s)}{rs} \mathrm{Re}[BF^*] - \frac{m_{B_c}^2 \lambda}{rs} \mathrm{Re}[CF^*] - \frac{m_{B_c}^2}{rs}(1-r)(1-r-s)\mathrm{Re}[BG^*] + \frac{m_{B_c}^4}{rs}\lambda(1-r)\mathrm{Re}[CG^*] - \frac{m_{B_c}^2}{r}(1-r-s)\mathrm{Re}[BH^*] + \frac{m_{B_c}^4 \lambda}{r}\mathrm{Re}[CH^*] \Big] \quad (22)$$

and the normal polarization by

$$P_N^- = \frac{1}{\Delta_{D_s^*}} m_{B_c}^3 m_\ell \pi \upsilon \sqrt{s\lambda} \Big[-4\,\mathrm{Im}[BE^*] - 4\,\mathrm{Im}[AF^*] + \frac{1}{r}(1-r-s)\,\mathrm{Im}[FH^*] + \frac{1}{r}(1+3r-s)\,\mathrm{Im}[FG^*] - \frac{1}{r} m_{B_c}^2 \lambda\,\mathrm{Im}[GH^*] \Big]. \quad (23)$$

We eliminate the dependence of the lepton polarizations on s in order to clarify the dependence on $1/R$, by considering the averaged forms over the allowed kinematical region. The averaged lepton polarizations are defined by

$$\langle P_i \rangle = \frac{\int_{(2m_\ell/m_{B_c})^2}^{(1-m_{D_s^*}/m_{B_c})^2} P_i \frac{d\mathcal{B}}{ds} ds}{\int_{(2m_\ell/m_{B_c})^2}^{(1-m_{D_s^*}/m_{B_c})^2} \frac{d\mathcal{B}}{ds} ds}. \quad (24)$$

The dependence of longitudinal polarizations on s with and without resonance contributions are given in Figs. 10

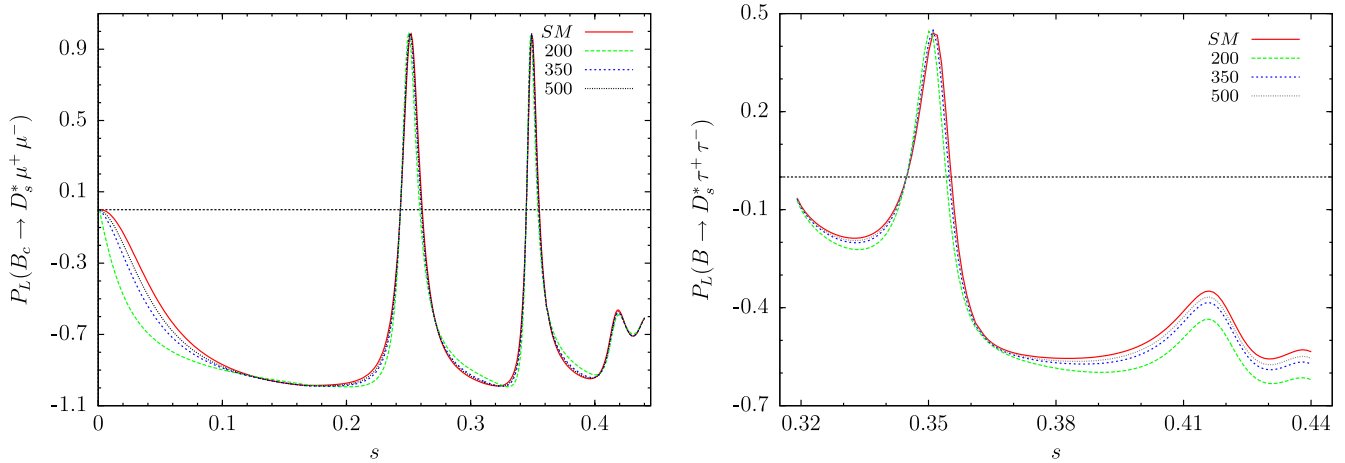

FIG. 11 (color online). The dependence of longitudinal polarization on s with resonance contributions using the central values of the form factors.

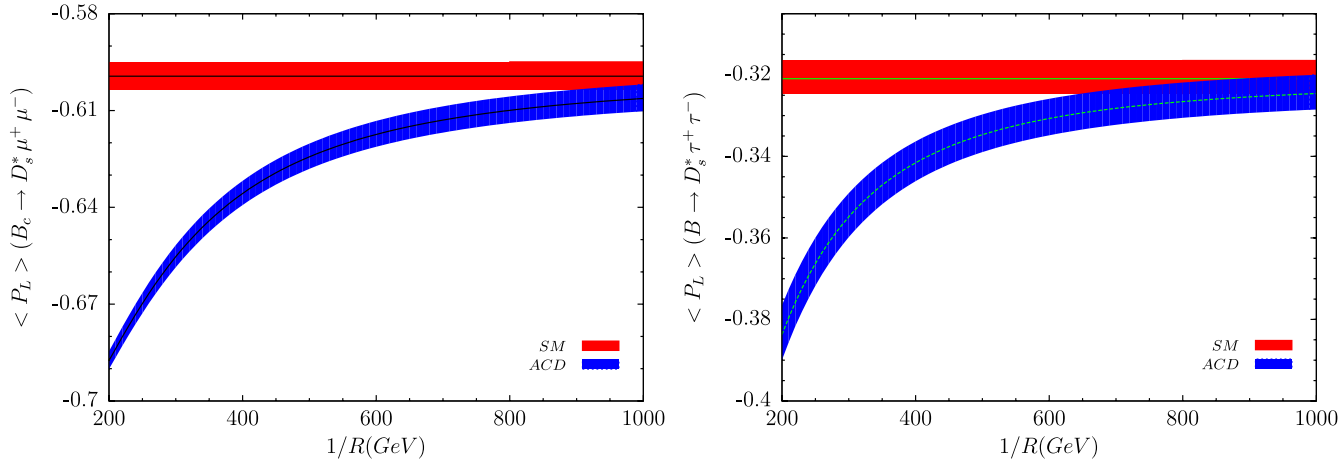

FIG. 12 (color online). The dependence of longitudinal polarization on $1/R$ including the uncertainty on the form factors and resonance contributions.

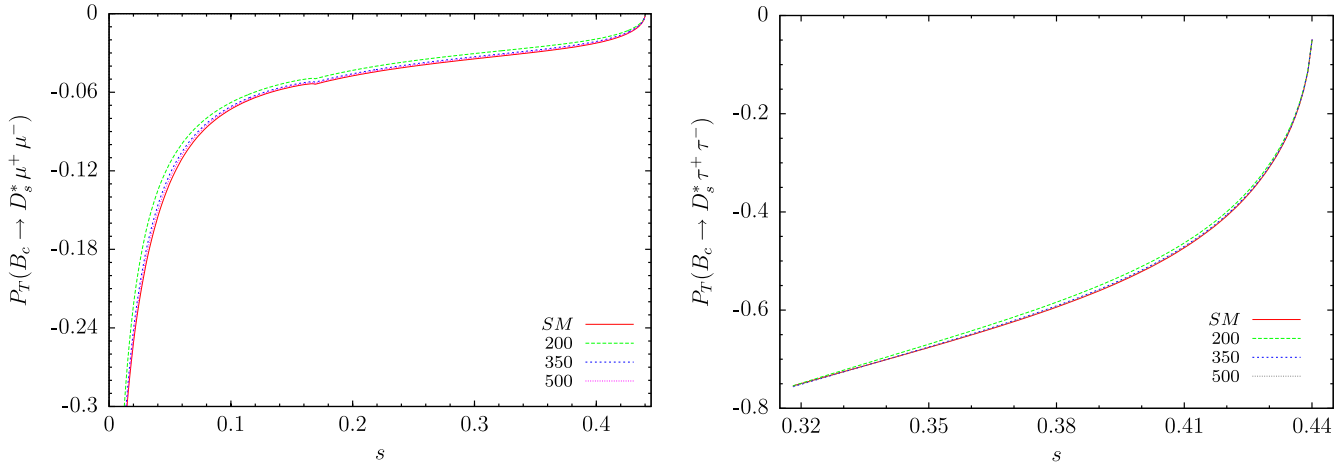

FIG. 13 (color online). The dependence of transversal polarization on s without resonance contributions using the central values of the form factors.

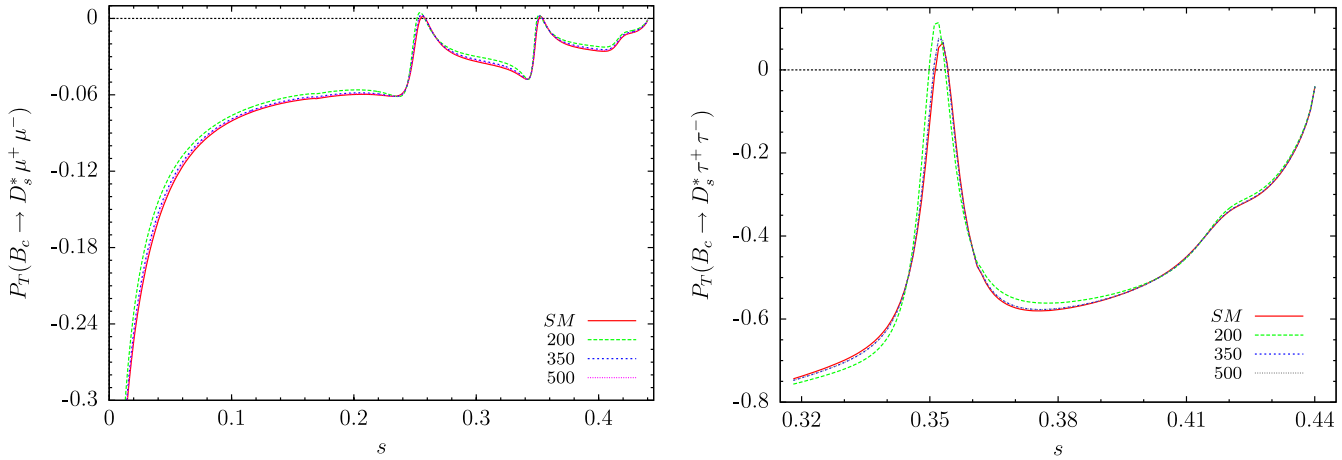

FIG. 14 (color online). The dependence of transversal polarization on s with resonance contributions using the central values of the form factors.

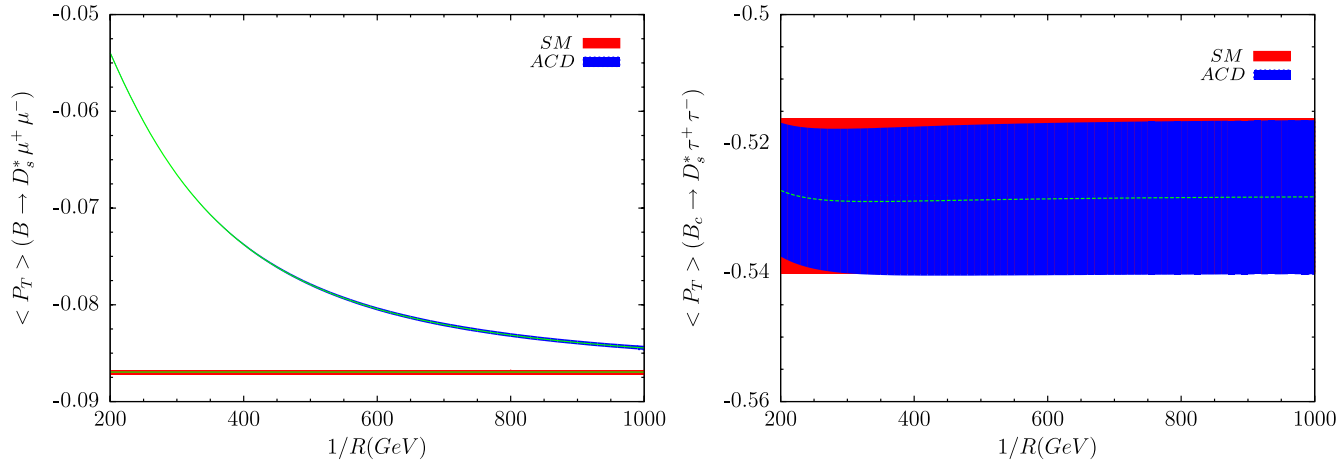

FIG. 15 (color online). The dependence of transversal polarization on $1/R$, including the uncertainty on the form factors.

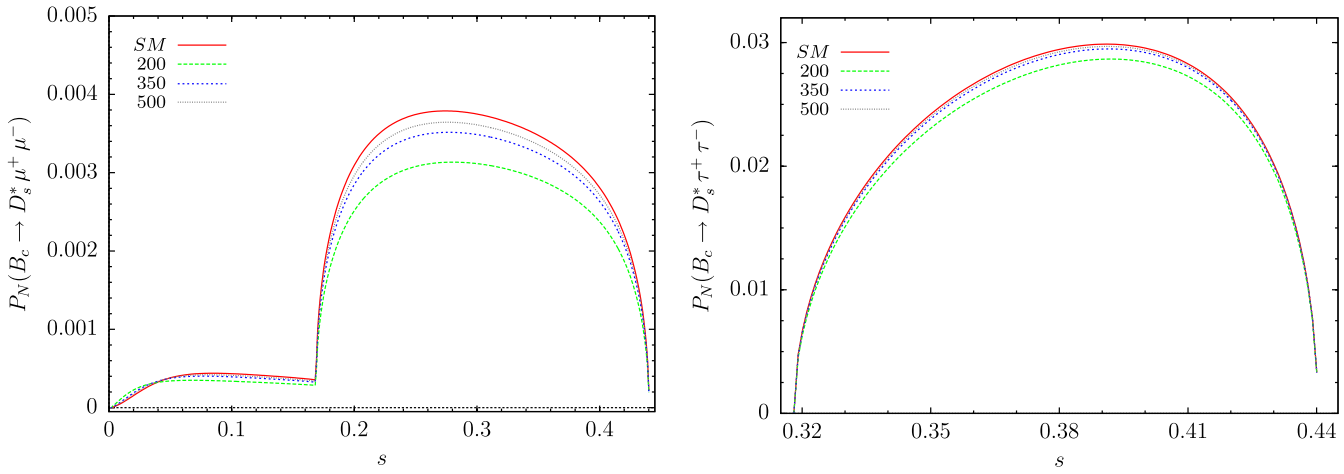

FIG. 16 (color online). The dependence of normal polarization on s with resonance contributions using the central values of the form factors.

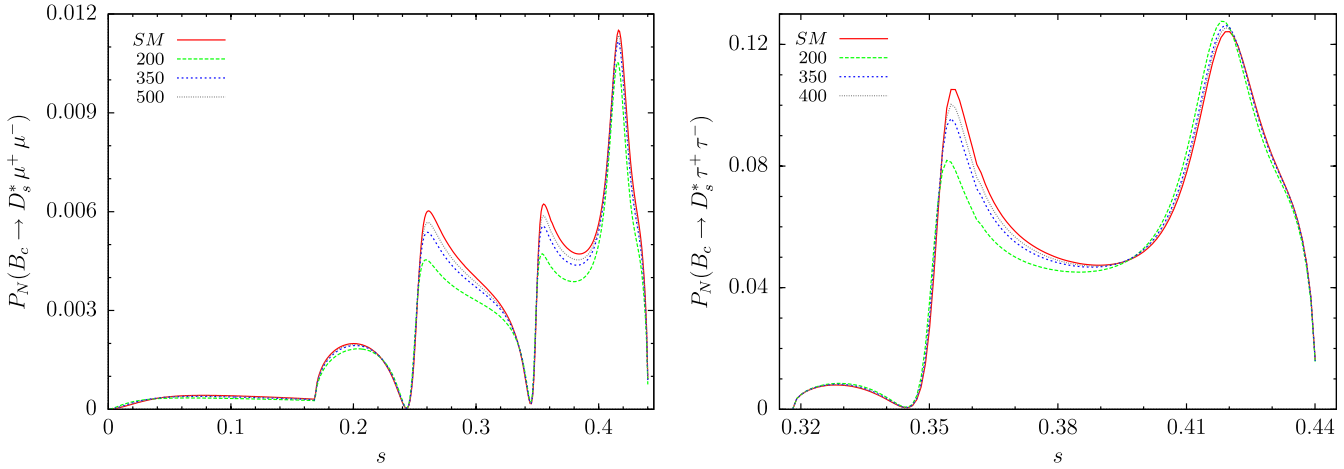

FIG. 17 (color online). The dependence of normal polarization on s without resonance contributions using the central values of the form factors.

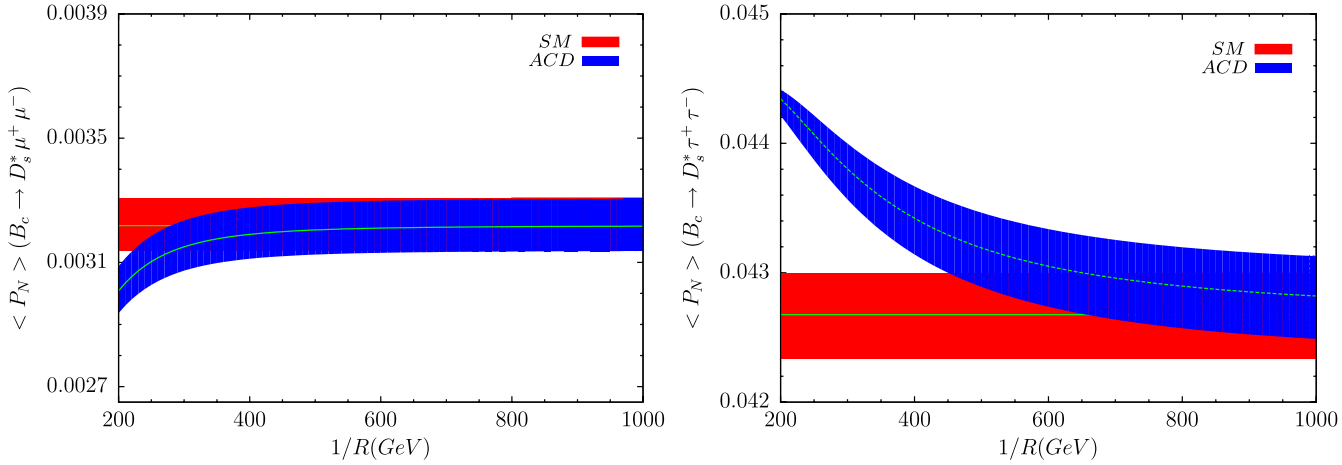

FIG. 18 (color online). The dependence of normal polarization on $1/R$ including the uncertainty on the form factors and resonance contributions.

and 11, respectively. For high values of s as $1/R$ approaches 200 GeV the deviation from the SM results become greater for τ in both the resonance and nonresonance cases, while for the μ channel this effect can be seen clearly for all s values when resonance contributions are not added; when including resonance contributions, around the peaks this effect seems to be suppressed and only for low values of s can we mention a deviation. Eliminating the dependence of the polarization on s, we get a variation of longitudinal polarizations with respect to $1/R$, given by Fig. 12. For $1/R \geq 500$ GeV, the difference becomes less important for both channels. The SM longitudinal polarization, $P_L = -0.599$, develops into $-0.670\,(-0.646)$ for $1/R = 250(350)$ GeV for μ. A similar aspect can also be noticed for τ. That is, the $P_L = -0.321$ SM value varies to $-0.366\,(-0.347)$ for $1/R = 250(350)$.

The dependence of transversal polarization on s with and without resonance contributions are given in Figs. 13 and 14, respectively. The UED effect is unimportant in both decay channels. In view of the $1/R$ dependency, given by Fig. 15, no difference is observed for the τ decay. Up to $1/R = 600$ GeV, the change is sizeable for the μ channel. In particular, between $1/R = 250$–350 GeV the difference might be checked for a signal of new physics.

We have plotted the variation of normal polarizations on s with and without resonance contributions in Figs. 16 and 17, respectively, and on $1/R$ in Fig. 18. The SM value itself for μ is tiny and as can be seen from the figures the effect of UED on normal polarization in this channel is irrelevant. Additionally, the relatively greater value of normal polarization in the SM for τ differs slightly.

VI. CONCLUSION

In this work, we discussed the $B_c \to D_s^* \ell^+ \ell^-$ decay for μ and τ as final state leptons in the SM and the ACD model. We used the form factors calculated in QCD sum rules and throughout the work, we reflected the errors in the form factors in the calculations and demonstrate the results in possible plotting.

Comparing the SM results and our theoretical predictions on the branching ratio for both decay channels, we obtain the lower bound as $1/R \sim 250$ GeV. Although this is consistent with the previously mentioned results, a detailed analysis, particularly with the data supplied by experiments, is necessary to put a precise bound on the compactification scale.

As an overall result, we can conclude that, as stated previous works in the literature, as $1/R \to 200$ GeV the physical values differ from the SM results. Up to a few hundreds GeV above the considered bounds, $1/R \geq 250$ GeV or $1/R \geq 350$ GeV, it is possible to see the effects of UED.

Taking the differential branching ratio into consideration, for small values of $1/R$ there is an essential difference compared with the SM results.

The difference between the SM and the ACD results in the forward-backward asymmetry of final state leptons, particularly in the specified region, the obtained result is essential. In addition, the position of the zero of forward-backward asymmetry, which is sensitive in searching new physics, can be a useful tool to check the UED contributions.

Polarizations of the leptons have been studied comprehensively and we found that transversal and normal polarizations are not sensitive to the extra dimension, only the dependence of transversal (normal) polarization on $1/R$ for the μ (τ) decay channel for low values of $1/R$ might be useful. However, studying longitudinal polarizations for both leptons up to $1/R = 600$ GeV will be a powerful tool in establishing new physics effects.

In the discussion throughout this work, the sizable discrepancies between the ACD model and the SM predictions at lower values of the compactification scale can be considered as indications of new physics and should be searched in the experiments.

ACKNOWLEDGMENTS

The author would like to thank K. Azizi for valuable discussion and U. Kanbur for contributions on computer based works.

APPENDIX: WILSON COEFFICIENTS IN THE ACD MODEL

In the ACD model, the new physics contributions appear by modifying available Wilson coefficients in the SM. The modified Wilson coefficients are calculated in [17,18] and can be expressed in terms of $F(x_t, 1/R)$ which generalize the corresponding SM functions $F_0(x_t)$ according to

$$F(x_t, 1/R) = F_0(x_t) + \sum_{n=1}^{\infty} F_n(x_t, x_n), \tag{A1}$$

where $x_t = m_t^2/m_W^2$, $x_n = m_n^2/m_W^2$ and $m_n = n/R$.

Instead of C_7, an effective, normalization scheme independent, coefficient C_7^{eff} in the leading logarithmic approximation is defined as

$$C_7^{\text{eff}}(\mu_b, 1/R) = \eta^{16/23} C_7(\mu_W, 1/R) + \frac{8}{3}(\eta^{14/23} - \eta^{16/23}) C_8 \times (\mu_W, 1/R) + C_2(\mu_W, 1/R) \sum_{i=1}^{8} h_i \eta^{a_i} \tag{A2}$$

with $\eta = \frac{\alpha_s(\mu_W)}{\alpha_s(\mu_b)}$ and

$$\alpha_s(x) = \frac{\alpha_s(m_Z)}{1 - \beta_0 \frac{\alpha_s(m_Z)}{2\pi} \ln(\frac{m_Z}{x})}, \tag{A3}$$

where in the fifth dimension $\alpha_s(m_Z) = 0.118$ and $\beta_0 = 23/3$.

The coefficients a_i and h_i are

$$a_i = (\tfrac{14}{23}, \tfrac{16}{23}, \tfrac{6}{23}, -\tfrac{12}{23}, 0.4086, -0.4230, -0.8994, 0.1456)$$
$$h_i = (2.2996, -1.088, -\tfrac{3}{7}, -\tfrac{1}{14}, -0.6494, -0.0380, -0.0186, -0.0057). \tag{A4}$$

The functions in (A2) are

$$C_2(\mu_W) = 1, \qquad C_7(\mu_W, 1/R) = -\tfrac{1}{2} D'(x_t, 1/R), \qquad C_8(\mu_W, 1/R) = -\tfrac{1}{2} E'(x_t, 1/R). \tag{A5}$$

Here, $D'(x_t, 1/R)$ and $E'(x_t, 1/R)$ are defined by using (A1) with the following functions:

$$D_0'(x_t) = -\frac{(8x_t^3 + 5x_t^2 - 7x_t)}{12(1 - x_t)^3} + \frac{x_t^2(2 - 3x_t)}{2(1 - x_t)^4} \ln x_t \tag{A6}$$

$$E_0'(x_t) = -\frac{x_t(x_t^2 - 5x_t - 2)}{4(1 - x_t)^3} + \frac{3x_t^2}{2(1 - x_t)^4} \ln x_t \tag{A7}$$

$$D_n'(x_t, x_n) = \frac{x_t(-37 + 44x_t + 17x_t^2 + 6x_n^2(10 - 9x_t + 3x_t^2) - 3x_n(21 - 54x_t + 17x_t^2))}{36(x_t - 1)^3} - \frac{(-2 + x_n + 3x_t)(x_t + 3x_t^2 + x_n^2(3 + x_t) - x_n(1 + (-10 + x_t)x_t))}{6(x_t - 1)^2} \ln\frac{x_n + x_t}{1 + x_n} + \frac{x_n(2 - 7x_n + 3x_n^2)}{6} \ln\frac{x_n}{1 + x_n} \tag{A8}$$

$$E_n'(x_t, x_n) = \frac{x_t(-17 - 8x_t + x_t^2 - 3x_n(21 - 6x_t + x_t^2) - 6x_n^2(10 - 9x_t + 3x_t^2))}{12(x_t - 1)^3} + \frac{(1 + x_n)(x_t + 3x_t^2 + x_n^2(3 + x_t) - x_n(1 + (-10 + x_t)x_t))}{2(x_t - 1)^4} \ln\frac{x_n + x_t}{1 + x_n} - \frac{1}{2} x_n(1 + x_n)(-1 + 3x_n) \ln\frac{x_n}{1 + x_n}. \tag{A9}$$

Following [17] or directly from [12] one gets the expressions for the sum over n as

$$\sum_{n=1}^{\infty} D_n'(x_t, x_n) = -\frac{x_t(-37 + x_t(44 + 17x_t))}{72(x_t - 1)^3} + \frac{\pi M_W R}{2}\Big[\int_0^1 dy \frac{(2y^{1/2} + 7y^{3/2} + 3y^{5/2})}{6} \coth(\pi M_W R\sqrt{y}) + \frac{(-2 + 3x_t)x_t(1 + 3x_t)}{6(x_t - 1)^4} J(R, -1/2) - \frac{1}{6(x_t - 1)^4}[x_t(1 + 3x_t) - (-2 + 3x_t)(1 + (-10 + x_t)x_t)] J(R, 1/2) + \frac{1}{6(x_t - 1)^4}[(-2 + 3x_t)(3 + x_t) - (1 + (-10 + x_t)x_t)] J(R, 3/2) - \frac{(3 + x_t)}{6(x_t - 1)^4} J(R, 5/2)\Big] \tag{A10}$$

and

$$\sum_{n=1}^{\infty} E_n'(x_t, x_n) = -\frac{x_t(-17 + (-8 + x_t)x_t)}{24(x_t - 1)^3} + \frac{\pi M_W R}{4}\Big[\int_0^1 dy(y^{1/2} + 2y^{3/2} - 3y^{5/2})\coth(\pi M_W R\sqrt{y}) - \frac{x_t(1 + 3x_t)}{(x_t - 1)^4}J(R, -1/2) + \frac{1}{(x_t - 1)^4}[x_t(1 + 3x_t) - (1 + (-10 + x_t)x_t)]J(R, 1/2) - \frac{1}{(x_t - 1)^4}[(3 + x_t) - (1 + (-10 + x_t)x_t)]J(R, 3/2) + \frac{(3 + x_t)}{(x_t - 1)^4}J(R, 5/2)\Big] \tag{A11}$$

where

$$J(R, \alpha) = \int_0^1 dy y^{\alpha}[\coth(\pi M_W R\sqrt{y}) - x_t^{1+\alpha}\coth(\pi m_t R\sqrt{y})]. \tag{A12}$$

The Wilson coefficient C_9 in the ACD model and the NDR scheme is

$$C_9(\mu, 1/R) = P_0^{\mathrm{NDR}} + \frac{Y(x_t, 1/R)}{\sin^2\theta_W} - 4Z(x_t, 1/R) + P_E E(x_t, 1/R), \tag{A13}$$

where $P_0^{\mathrm{NDR}} = 2.6 \pm 0.25$ and P_E is numerically negligible. The functions $Y(x_t, 1/R)$ and $Z(x_t, 1/R)$ are defined as

$$Y(x_t, 1/R) = Y_0(x_t) + \sum_{n=1}^{\infty} C_n(x_t, x_n) \tag{A14}$$

$$Z(x_t, 1/R) = Z_0(x_t) + \sum_{n=1}^{\infty} C_n(x_t, x_n), \tag{A15}$$

with

$$Y_0(x_t) = \frac{x_t}{8}\Big[\frac{x_t - 4}{x_t - 1} + \frac{3x_t}{(x_t - 1)^2}\ln x_t\Big] \tag{A16}$$

$$Z_0(x_t) = \frac{18x_t^4 - 163x_t^3 + 259x_t^2 - 108x_t}{144(x_t - 1)^3} + \Big[\frac{32x_t^4 - 38x_t^3 - 15x_t^2 + 18x_t}{72(x_t - 1)^4} - \frac{1}{9}\Big]\ln x_t \tag{A17}$$

$$C_n(x_t, x_n) = \frac{x_t}{8(x_t - 1)^2}\Big[x_t^2 - 8x_t + 7 + (3 + 3x_t + 7x_n - x_t x_n)\ln\frac{x_t + x_n}{1 + x_n}\Big] \tag{A18}$$

and

$$\sum_{n=1}^{\infty} C_n(x_t, x_n) = \frac{x_t(7 - x_t)}{16(x_t - 1)} - \frac{\pi M_W R x_t}{16(x_t - 1)^2}[3(1 + x_t)J(R, -1/2) + (x_t - 7)J(R, 1/2)]. \tag{A19}$$

The μ independent C_{10} is given by

$$C_{10}(1/R) = -\frac{Y(x_t, 1/R)}{\sin^2\theta_W} \tag{A20}$$

where $Y(x_t, 1/R)$ is defined in (A14).

[1] M. S. Alam *et al.* (CLEO Collaboration), Phys. Rev. Lett. **74**, 2885 (1995).
[2] A. Ali, Int. J. Mod. Phys. A **20**, 5080 (2005).
[3] F. Abe *et al.* (CDF Collaboration), Phys. Rev. D **58**, 112004 (1998).
[4] J. Sun, Y. Yang, W. Du, and H. Ma, Phys. Rev. D **77**, 114004 (2008).
[5] M. P. Altarelli and F. Teubert, Int. J. Mod. Phys. A **23**, 5117 (2008).
[6] I. Antoniadis, Phys. Lett. B **246**, 377 (1990).

[7] I. Antoniadis, N. Arkani-Hamed, S. Dimopoulos, and G. Dvali, Phys. Lett. B **436**, 257 (1998).
[8] N. Arkani-Hamed, S. Dimopoulos, and G. Dvali, Phys. Lett. B **429**, 263 (1998).
[9] N. Arkani-Hamed, S. Dimopoulos, and G. Dvali, Phys. Rev. D **59**, 086004 (1999).
[10] T. Appelquist, H. C. Cheng, and B. A. Dobrescu, Phys. Rev. D **64**, 035002 (2001).
[11] K. Agashe, N. G. Deshpande, and G. H. Wu, Phys. Lett. B **511**, 85 (2001); **514**, 309 (2001).
[12] P. Colangelo, F. De Fazio, R. Ferrandes, and T. N. Pham, Phys. Rev. D **73**, 115006 (2006).
[13] U. Haisch and A. Weiler, Phys. Rev. D **76**, 034014 (2007).
[14] P. Biancofiore, P. Colangelo, and F. Fazio, Phys. Rev. D **85**, 094012 (2012).
[15] T. Aaltonen *et al.* (CDF Collaboration), Phys. Rev. Lett. **107**, 201802 (2011).
[16] K. Azizi S. Kartal, N. Katırcı, A. T. Olgun, and Z. Tavukog lu, J. High Energy Phys. 05 (2012) 024.
[17] A. J. Buras, M. Spranger, and A. Weiler, Nucl. Phys. **B660**, 225 (2003).
[18] A. J. Buras, A. Poschenrieder, M. Spranger, and A. Weiler, Nucl. Phys. **B678**, 455 (2004).
[19] P. Colangelo, F. De Fazio, R. Ferrandes, and T. N. Pham, Phys. Rev. D **74**, 115006 (2006).
[20] G. Devidze, A. Liparteliani, and U. G. Meissner, Phys. Lett. B **634**, 59 (2006).
[21] T. M. Aliev and M. Savci, Eur. Phys. J. C **50**, 91 (2007).
[22] R. Mohanta and A. K. Giri, Phys. Rev. D **75**, 035008 (2007).
[23] P. Colangelo, F. De Fazio, R. Ferrandes, and T. N. Pham, Phys. Rev. D **77**, 055019 (2008).
[24] A. Saddique, M. J. Aslam, and C. D. Lu, Eur. Phys. J. C **56**, 267 (2008).
[25] I. Ahmed, M. A. Paracha, and M. J. Aslam, Eur. Phys. J. C **54**, 591 (2008).
[26] V. Bashiry and K. Zeynali, Phys. Rev. D **79**, 033006 (2009).
[27] N. Katirci and K. Azizi, J. High Energy Phys. 01 (2011) 087.
[28] N. Katirci and K. Azizi, J. High Energy Phys. 07 (2011) 043.
[29] Y. Li and J. Hua, Eur. Phys. J. C **71**, 1764 (2011).
[30] U. O. Yilmaz and G. Turan, Eur. Phys. J. C **51**, 63 (2007).
[31] A. Ahmed I. Ahmed, M. A. Paracha, M. Junaid, A. Rehman, and M. J. Aslam, arXiv:1108.1058v3.
[32] I. Ahmed M. A. Paracha, M. Junaid, A. Ahmed, A. Rehman, and M. J. Aslam, arXiv:1107.5694v2.
[33] M. A. Paracha, I. Ahmed, and M. J. Aslam, Phys. Rev. D **84**, 035003 (2011).
[34] C. Q. Geng, C. W. Hwang, and C. C. Liu, Phys. Rev. D **65**, 094037 (2002).
[35] A. Faessler, Th. Gutsche, M. A. Ivanov, J. G. Körner, and V. E. Lyubovitskij, Eur. Phys. J. direct C **4**, 18 (2002).
[36] D. Ebert, R. N. Faustov, and V. O. Galkin, Phys. Rev. D **82**, 034032 (2010).
[37] T. Wang, D.-X. Zhang, B.-Q. Ma, and T. Liu, Eur. Phys. J. C **71**, 1758 (2011).
[38] K. Azizi, F. Falahati, V. Bashiry, and S. M. Zebarjad, Phys. Rev. D **77**, 114024 (2008).
[39] G. Buchalla, A. J. Buras, and M. Lautenbacher, Rev. Mod. Phys. **68**, 1125 (1996).
[40] A. J. Buras and M. Münz, Phys. Rev. D **52**, 186 (1995).
[41] M. Misiak, Nucl. Phys. **B393**, 23 (1993); **B439**, 461(E) (1995).
[42] A. Ali, T. Mannel, and T. Morozumi, Phys. Lett. B **273**, 505 (1991).
[43] K. Nakamura *et al.* (Particle Data Group), J. Phys. G **37**, 075021 (2010).
[44] A. Ali, P. Ball, L. T. Handoko, and G. Hiller, Phys. Rev. D **61**, 074024 (2000).
[45] P. Ball and R. Zwicky, Phys. Rev. D **71**, 014029 (2005).
[46] G. Erkol and G. Turan, Eur. Phys. J. C **25**, 575 (2002).
[47] S. Fukae, C. S. Kim, and T. Yoshikawa, Phys. Rev. D **61**, 074015 (2000).
[48] F. Krüger and L. M. Sehgal, Phys. Lett. B **380**, 199 (1996).